IOP Publishing Physica Scripta
Phys. Scr. 95 (2020) 045702 (12pp) https://doi.org/10.1088/1402-4896/ab5e95

Spin domains in ground state of a trapped spin-1 condensate: a general study under Thomas–Fermi approximation

Projjwal K Kanjilal[1] **and A Bhattacharyay**

Indian Institute of Science Education and Research, Pune, India

E-mail: projjwal.kanjilal@students.iiserpune.ac.in and a.bhattacharyay@iiserpune.ac.in

Received 4 September 2019, revised 19 November 2019
Accepted for publication 4 December 2019
Published 12 February 2020

Abstract

Investigation of ground state structures and phase separation under confinement is of great interest in spinor Bose–Einstein condensates. In this paper we show that, in general, within the Thomas–Fermi approximation, the phase separation scenario of stationary states can be obtained including all the mixed states on an equal footing for a spin-1 condensate under any confinement. According to the process used here, the density of each and every stationary states can be determined exactly in terms of the system parameters. This allows to write the expression for energy density of all states in a form which are not an explicit function of densities of those states. An energy density comparison therefore, among all the allowed stationary states can be done which will reveal domain structures depending on the system parameters. We study here, in details, a particular case of spherically symmetric harmonic confinement as an example and show a wide range of potential phase separation scenario for anti-ferromagnetic and ferromagnetic interactions.

Keywords: phase separation, domain formation, spinor Bose–Einstein condensate

1. Introduction

Phase separation of multicomponent Bose–Einstein condensate (BEC) under trapping, as opposed to the phase separation which does not require external fields, was theoretically investigated by Timmermans [1] who named it 'potential separation'. Spin domain formation in an optically trapped sodium spinor condensate has been reported by Stenger *et al*, [2] followed by a detailed theoretical justification by Isoshima *et al* [3]. A number of theoretical investigations have followed since then to describe the spin domain formation of trapped spin-1 condensate in many different ways [4–7], even at zero magnetic field [8, 9]. T-L Ho and VB Shenoy have given a detailed picture of binary condensates, for which phase separation arises due to the interplay between intra- and inter-species interaction [10]. This led to a lot of scientific interest to explore many possible scenarios of domain formation for binary condensates [11–20]. In recent years a lot of thorough scientific investigations have provided the ground state structure and a detailed picture of instability induced phase separation in a spin orbit coupled condensate [21–25].

To find out the spin domain formation in the ground state of a spinor BEC, Thomas–Fermi (T–F) approximation is extensively used [3, 10, 18, 26, 27] where the spatial derivatives of order parameter are neglected. This is an approximation where one neglects the kinetic energy term on the basis of considering slow or large length scale spatial variation of the order parameter. This is a reasonable first step to understand phase separation under entrapment when the trap size is bigger than the healing length [4]. This procedure provides a wider picture of all possibilities out of which some scenarios might not be present due to instabilities arising from various conditions. However, irrespective of the presence of these instabilities of the stationary states, as a first step, getting a complete picture of coexisting stationary phases in the ground state is desirable.

In this paper we follow the T–F approximation to exhaustively investigate the possible phase separations of stationary states under confinement. We show here that, the T–F approximation allows for an exact expression of the

[1] Author to whom any correspondence should be addressed.

energy density of all the possible stationary phases in terms of confining potential and the parameters of the system. This allows for a direct comparison of energy densities of all possible phases on an equal footing at a constant chemical potential to determine which phase is locally of the lowest energy. This becomes possible under the T–F approximation because the energy density can be written as a function of the exactly determined local total density of the system irrespective of particular phases present.

The wider context of research on spinor BEC rests on the fact that the condensate order parameter having $2f + 1$ components (for a spin-f system) the BEC can generate a host of purely quantum mechanical complexities in the static as well as dynamic manifestations. The experimental ability of very fine tuning of parameters coupled to this potential variety of quantum phenomena provides a unique window of opportunity to observe and understand many body quantum phenomena [28, 29]. The first step towards standardizing such machinery would be achieving a concise description of all the competing ground states of the system possibly over the whole allowed parameter space. To this end, given the nonlinear nature of even the mean field (GP) dynamics, T–F approximated approach can give a unified description. Although there exists a considerable amount of literature addressing mean field description of spin domain formation in spinor BEC, it was not foreseen in the existing literature that under the single constraint of constant chemical potential the GP dynamics in T–F approximation can actually capture whole spectrum of phase co-existence scenarios for any general confinement. This very general and exact method is being shown in the present paper. Since this general procedure shows result over the whole range of relevant parameters and for any confining potential $U(\vec{r})$, this would be useful information for parameter setting in future experiments and simulations.

On the basis of exact calculations we show here that T–F approximation produces some interesting results. In the presence of anti-ferromagnetic interactions the potential phase separation does not involve anti-ferromagnetic phases over a very wide range of parameters. This situation is dominated by domain formation involving ferromagnetic stationary phases. Three-phase domain formation is only observed when the interactions are anti-ferromagnetic. When the spin–spin interaction is ferromagnetic, under T–F approximation, there actually appears no domain formation involving ferromagnetic phase over a very wide parameter space that we have explored under isotropic harmonic confinement. Rather the anti-ferromagnetic and polar phases dominate along with the phase-matched (PM) and anti-phase-matched (APM) (1,1,1) phases. However, at Zeeman coupling more than ± 150 Hz, ferromagnetic phase starts dominating. In this article, the energy unit is Hz, which is calculated by dividing the SI unit of energy with h, the Planck's constant.

Regarding the nomenclature we use binary notation 1 for filled spin subcomponent and 0 for empty one. For example, the anti-ferromagnetic phase with filled $m_z = \pm 1$ and empty $m_z = 0$ components would be denoted as (1, 0, 1), where m_z is the projection of spin-1 particle along z axis. The (1, 1, 1) phase indicates presence of all the spin components and would be seen to dominate quite a lot of the domain formation scenarios along with the mixed phases (0, 1, 1) and (1, 1, 0).

After establishing energy densities for a general confining potential $U(\vec{r})$, we show the domain structures here for a special case of the $U(\vec{r})$, an isotropic harmonic confinement $U(r) = \frac{1}{2}\omega r^2$. However, the same analysis can be used to include any potential and can be extended to effectively 2-dimensional or 1-dimensional systems. GP dynamics for effective 2- and 1-dimensional systems are obtained by integrating out the dimensions which are confined below the healing length. This essentially gives back the same structure of GP model with renormalized couplings where the length scales of the confined dimensions feature [8]. The same structure of the GP model in all these dimensions makes it amenable to the general method presented in this paper.

The chemical potentials of the basic Zeeman components (1,0,0), (0,1,0) and (0,0,1) are constrained to remain constant for the chemical stability of the co-existing domains and the mixed states. This is a minimal condition, that has to be strictly adhered to in the analysis of phase co-existence. For anti-ferromagnetic and ferromagnetic cases we fix parameters corresponding to ^{23}Na and ^{87}Rb respectively [26, 30].

The plan of the paper is as follows. We begin with the description of the standard mean field analysis using Gross–Pitaevskii equation for a spin-1 BEC and reproduce the phase diagrams of the unconfined case following standard literature. Then we show the phase separations in the confined case where the spin–spin interaction is negligible and compare some of these results with those of the unconfined case. A detailed description of phase separation for the anti-ferromagnetic and the ferromagnetic cases follows in the next subsections. We then present a discussion of our results.

2. Mean field dynamics of the condensate

The dynamics of spin-1 condensate under mean field approximation is given by Gross–Pitaevskii equation [27, 28, 31]

$$\mathrm{i}\hbar\frac{\partial\psi_m}{\partial t} = (\mathcal{H} - pm + qm^2)\psi_m + c_1\sum_{m'=-1}^{1}\vec{F}.\vec{f}_{mm'}\psi_{m'}, \quad (1)$$

where the $\mathcal{H}$ corresponds to the symmetric part of the Hamiltonian, $\mathcal{H} = -\frac{\hbar^2\nabla^2}{2M} + U(\vec{r}) + c_0 n$ and the suffix m and m' take values -1, 0, 1. The spin matrices are given by

$$f_x = \frac{1}{\sqrt{2}}\begin{bmatrix}0 & 1 & 0\\ 1 & 0 & 1\\ 0 & 1 & 0\end{bmatrix}, f_y = \frac{\mathrm{i}}{\sqrt{2}}\begin{bmatrix}0 & -1 & 0\\ 1 & 0 & -1\\ 0 & 1 & 0\end{bmatrix},$$
$$f_z = \begin{bmatrix}1 & 0 & 0\\ 0 & 0 & 0\\ 0 & 0 & -1\end{bmatrix}.$$

ψ_m is the order parameter corresponding to the mth spin component and $|\psi_m|^2 = n_m$ gives the density of corresponding spin component. The total density $n = n_1 + n_0 + n_{-1}$ is the constraint existing everywhere over space. $U(\vec{r})$ is, in general, a three dimensional trapping potential and M is the

mass of a boson. The parameter p sets the strength of the Zeeman term where, $p = -g\mu_B$B. Here g is the Lande hyperfine g-factor, μ_B is the Bohr magneton and the magnetic field is applied along the z axis (say) to lift the degeneracy of the spin states. The parameter q is the strength of the quadratic Zeeman term where, $q = (g\mu_B B)^2/\Delta\, E_{hf}$ with $\Delta\, E_{hf}$ is the hyperfine splitting. In the above equation, $\vec{F}$ is local spin density vector defined as

$$F_l(\vec{r}) = \sum_{m,m'=-1}^{1} \psi_m^*(\vec{r})(f_l)_{mm'}\psi_{m'}(\vec{r}), \tag{2}$$

where $l = x, y, z$. It can be understood that the coefficient of the linear Zeeman term p can include the additive Lagrange multiplier arising from the conservation of magnetization which might be there due to the presence of a magnetic field and total spin orientation conserving scattering. The constants $c_1 = \frac{4\pi\hbar^2}{M}\frac{(a_2 - a_0)}{3}$, $c_0 = \frac{4\pi\hbar^2}{M}\frac{(2a_2 + a_0)}{3}$, where a_0 and a_2 are the s wave scattering lengths for hyperfine spin channels 0 and 2 respectively. Typical values of these scattering lengths in atomic units for ^{23}Na $a_2 = 52.98 \pm 0.40a.u.$, $a_0 = 47.36 \pm 0.80a.u.$ and for ^{87}Rb are $a_2 = 100.40 \pm 0.10a.u.$, $a_0 = 101.8 \pm 0.20a.u.$, [28]. In what follows, these typical values will be used for ferro- and anti-ferromagnetic cases of analysis.

More explicitly, the components of the spin density vectors are

$$F_x = \frac{1}{\sqrt{2}}[\psi_{-1}^*\psi_0 + \psi_1^*\psi_0 + \psi_0^*(\psi_{-1} + \psi_1)], \tag{3}$$

$$F_y = \frac{\mathrm{i}}{\sqrt{2}}[\psi_{-1}^*\psi_0 - \psi_1^*\psi_0 + \psi_0^*(\psi_1 - \psi_{-1})], \tag{4}$$

$$F_z = \psi_1^*\psi_1 - \psi_{-1}^*\psi_{-1}. \tag{5}$$

The mean-field energy of this system can always be written as

$$E[\psi] = \langle\hat{H}\rangle_0 = \int \mathrm{d}\vec{r}\, e(\vec{r}), \tag{6}$$

where the local energy density $e(\vec{r})$ is the central quantity which will determine the phase diagrams for a confined system. Explicit expression of the local energy density would read as

$$e(\vec{r}) = \sum_{m=-1}^{1} \psi_m^*\left[-\frac{\hbar^2\nabla^2}{2M} + U_{\mathrm{trap}}(\vec{r}) - pm + qm^2\right]\psi_m + \frac{c_0}{2}n^2 + \frac{c_1}{2}|\vec{F}|^2. \tag{7}$$

A detailed phase diagram of the free system i.e. when $U(\vec{r}) = 0$ is well described in the review [28] where going by the ansatz

$$\psi_m(\vec{r}, t) = \sqrt{n}\,\zeta_m \mathrm{e}^{-\mathrm{i}\mu t/\hbar}, \tag{8}$$

setting ζ_0 real and $Im(\zeta_{+1}) = Im(\zeta_{-1})$ by fixing of the overall phase, the following phase diagrams were arrived (figure 1).

These phase diagrams (figure 1) capture five distinct phases separated by boundaries which are functions of the parameters p, q, c_1 and the density n of the condensate in the presence of a magnetic field. These mean field phase diagrams have been immensely useful in understanding many experimental results [2]. These diagrams, practically at the zero temperature of the condensate, indicate a set of (quantum) phase transition boundaries as a function of density. For a trapped BEC, the constant density condition underlying the analysis of a free condensate is no longer valid. Phase separation, therefore, can arise in a trapped spinor condensate as a function of density. We are going to systematically capture in this paper a complete and coherent mean-field description of phase separation and domain formation of trapped spin-1 condensate.

3. Phase separation of the trapped condensate

In the presence of trapping potential $U(\vec{r})$ the GP dynamics of the spinor gas of spin-1 can be decomposed into parts by taking the ansatz

$$\psi_m(\vec{r}, t) = \sqrt{n_m(\vec{r})}\exp(-\frac{\mathrm{i}\mu t}{\hbar})\exp(-\mathrm{i}\theta_m). \tag{9}$$

The relative phase being defined as $\theta_r = \theta_1 + \theta_{-1} - 2\theta_0$, the dynamics of amplitudes and phases are

$$\dot{n}_0(\vec{r}) = -\frac{4c_1 n_0\sqrt{n_1 n_{-1}}\sin\theta_r}{\hbar}, \tag{10}$$

$$\dot{n}_{\pm1}(\vec{r}) = \frac{2c_1 n_0\sqrt{n_1 n_{-1}}\sin\theta_r}{\hbar}, \tag{11}$$

$$\hbar\dot{\theta}_0 = \frac{1}{\sqrt{n_0(\vec{r})}}(\mathcal{H} - \mu)\sqrt{n_0(\vec{r})} + c_1(n_1 + n_{-1} + 2\sqrt{n_{-1}n_1}\cos\theta_r), \tag{12}$$

$$\hbar\dot{\theta}_{\pm1} = \frac{1}{\sqrt{n_{\pm1}(\vec{r})}}(\mathcal{H} - \mu)\sqrt{n_{\pm1}(\vec{r})} \pm c_1(n_1 - n_{-1}) + q \mp p + c_1 n_0\left(1 + \sqrt{\frac{n_{\mp1}(\vec{r})}{n_{\pm1}(\vec{r})}}\cos\theta_r\right); \tag{13}$$

where $\mathcal{H} = -\frac{\hbar^2\nabla^2}{2M} + U(\vec{r}) + c_0 n$.

The phase matching condition demands $\mu_+ + \mu_- = 2\mu_0$, which is valid even when $\mu_+ = \mu_- = \mu_0$. μ's are the corresponding chemical potential and stability of the mixed phases would require them to remain constant. In what follows, we will always impose this condition of the constant chemical potential μ in order to have chemical stability of the co-existing

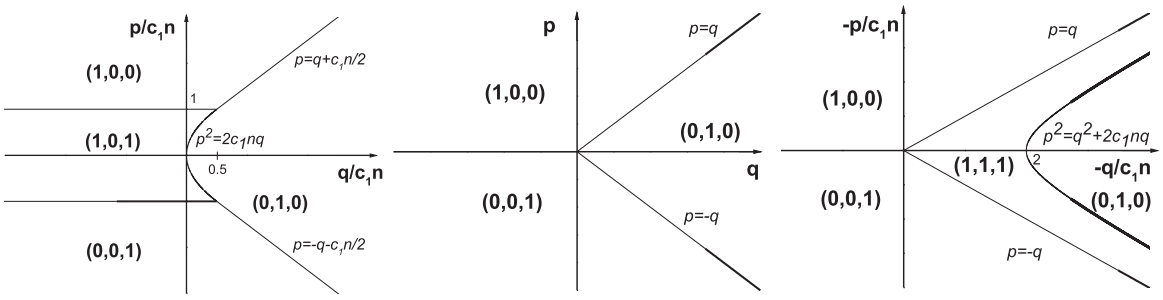

(a) $c_1 > 0$ (b) $c_1 = 0$ (c) $c_1 < 0$

Figure 1. Phase diagram in (p,q) parametric space of a spin-1 BEC in free space. The linear and quadratic Zeeman terms are represented as p and q respectively. These phase diagrams are particularly useful to determine the ground state structures of a homogeneous spin-1 condensate with (a) anti-ferromagnetic, (b) no spin–spin and (c) ferromagnetic interactions.

Table 1. Stationary states at $c_1 = 0$. Associated conditions for the last four states are $p = q$, $p = 0$, $p = -q$ and $p = 0$, $q = 0$ respectively. The energy density expressions shown in this table for all the stationary states are obtained from equation (7) by substituting specific density profiles. Here F is an abbreviation for ferromagnetic states and P is that for polar state.

States	Variation of density	Energy density	Restriction
(1, 0, 0) F1	$c_0 n(\vec{r}) = \mu + p - q - U(\vec{r})$	$e_1 = \frac{[U(\vec{r})-p+q][\mu+p-q-U(\vec{r})]}{c_0} + \frac{[\mu+p-q-U(\vec{r})]^2}{2c_0}$	none
(0, 1, 0) P	$c_0 n(\vec{r}) = \mu - U(\vec{r})$	$e_2 = \frac{U(\vec{r})[\mu-U(\vec{r})]}{c_0} + \frac{[\mu-U(\vec{r})]^2}{2c_0}$	none
(0, 0, 1) F2	$c_0 n(\vec{r}) = \mu - p - q - U(\vec{r})$	$e_3 = \frac{[U(\vec{r})+p+q][\mu-p-q-U(\vec{r})]}{c_0} + \frac{[\mu-p-q-U(\vec{r})]^2}{2c_0}$	none
(1, 1, 0)	$c_0 n(\vec{r}) = \mu - U(\vec{r})$	$e_4 = \frac{U(\vec{r})[\mu-U(\vec{r})]}{c_0} + \frac{[\mu-U(\vec{r})]^2}{2c_0}$	$p = q$
(1, 0, 1)	$c_0 n(\vec{r}) = \mu - q - U(\vec{r})$	$e_5 = \frac{[U(\vec{r})+q][\mu-q-U(\vec{r})]}{c_0} + \frac{[\mu-q-U(\vec{r})]^2}{2c_0}$	$p = 0$
(0, 1, 1)	$c_0 n(\vec{r}) = \mu - U(\vec{r})$	$e_6 = \frac{U(\vec{r})[\mu-U(\vec{r})]}{c_0} + \frac{[\mu-U(\vec{r})]^2}{2c_0}$	$p = -q$
(1, 1, 1)	$c_0 n(\vec{r}) = \mu - U(\vec{r})$	$e_7 = \frac{U(\vec{r})[\mu-U(\vec{r})]}{c_0} + \frac{[\mu-U(\vec{r})]^2}{2c_0}$	$p = q = 0$

phases. The relative phase θ_r and individual phases θ_m's are treated as global parameters, the dynamics of which actually hold the key of the relative energy of the various spin phases, that we are going to look for, on an equal footing. In this particular work we are investigating states which have either a constant phase over space or the phase gradients are negligible; otherwise, vortex solutions can also emerge as ground state [32] which we are not considering in this paper.

3.1. Phase separation for $c_1 = 0$

The condition, $c_1 \simeq 0$ incorporates almost no interaction of spins. This is the situation sitting at the boundary of the two broad regimes namely $c_1 > 0$ (anti-ferromagnetic) and $c_1 < 0$ (ferromagnetic). We follow here the standard scheme of dividing the parameter regime of spin interactions as is done for the free condensate [28] to have a direct comparison. Setting $c_1 = 0$, one can now easily get the corresponding energy densities of the seven basic spin configurations in terms of the total density under T–F approximation (i.e. spatial derivatives of density and phases are neglected). As an example let us explore the anti-ferromagnetic state, (1, 0, 1). As $n_0 = 0$ here, equation (12) is no longer valid and the solution should obey the stationarity of other two sub-component phases resulting in

$$U(\vec{r}) + c_0 n - \mu \mp p + q = 0, \tag{14}$$

when $n = n_1 + n_{-1}$. Note that, equation (13) take such a simple form because we are studying the case where spin dependent interaction is absent. From equation (14) it is easy to see that the T–F profile for the (1, 0, 1) state would be

$$c_0 n(\vec{r}) = \mu - q - U(\vec{r}), \tag{15}$$

when $p = 0$. Here $p = 0$ is the condition for existence of this phase. Following the similar scheme would allow one to find the T–F profile, corresponding energy density and the parameter restrictions for all the stationary states summarized in table 1.

Note that, all the restrictions present on the parameters corresponding to the last four phases in the table which are $p = q, p = 0, p = -q$ and $p = q = 0$ arise from the solution of equations (12)–(13). An immediate consequence of these parameter restrictions is that, except for the case i.e. $p = q = 0$, the states (1, 1, 0), (1, 0, 1) and (0, 1, 1) cannot exist together. So there is no domain formation for these phases anywhere over the p versus q parameter plane except at the origin. The phase (1, 1, 1) exists only at the origin on this plane as well.

Figure 2(a) is a phase diagram showing which one of the first three phases (1, 0, 0), (0, 1, 0) and (0, 0, 1) exists where on the p *versus* q plane at $c_1 = 0$. This gives us a clear idea as to where on this phase diagram the domain formation can be expected depending upon any particular form of the

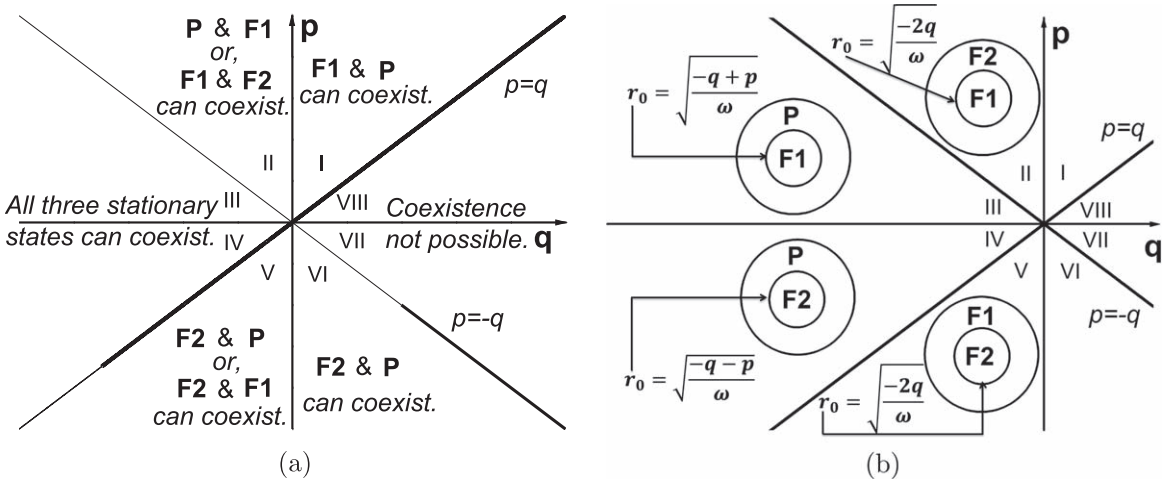

Figure 2. Co-existing phases and domain formation in (p, q) parameter space of trapped spin-1 BEC for $c_1 = 0$. The states (1, 0, 0), (0, 0, 1) and (0, 1, 0) are represented by F1, F2 and P for better visibility. For a uniform two dimensional harmonic trap the phase-separation radius (r_0) from the centre of the trap is shown as well.

trapping potential $U(\vec{r})$ which is considered to be harmonic here. The diagonal lines, the $q - axis$ and the origin are the places where the other four phases namely (1, 1, 0), (1, 0, 1), (0, 1, 1) and (1, 1, 1) exist. An actual pair-wise comparison of energy densities shows the inner and the outer phases to expect in a harmonic trap in the region for negative q in figure 2(b). This figure also includes an estimation of the radius of phase boundaries under harmonic confinement. The same comparison is sufficient to deduce that no phase separation or domain formation is possible for $q > 0$.

To look at an example for the formation of domains when $U(\vec{r}) = \frac{1}{2}\omega r^2$ is a harmonic trapping, let us choose the region (III) where first three single component phases can exist. A comparison of energy densities of the (1, 0, 0) and (0, 1, 0) shows that

$$\Delta e_{12} \equiv e_1 - e_2 = \frac{(p-q)[2U(\vec{r}) - (p-q)]}{2c_0} \qquad (16)$$

and it implies that the state (1, 0, 0) energetically is favored below a radius $r_0^2 = (p-q)/\omega$ because $(p-q) > 0$. The state (0, 1, 0) should be existing for $r > r_0$ and is the peripheral state when (1, 0, 0) sits at the core of the harmonic trap. The situation does not happen when $(p-q)$ is negative as the radius becomes imaginary. The same reason is enough to understand that phase separation between the F1 and P is only possible in region-I, II, III and IV of figure 2(a). All such comparison can now be done and one gets the ground state domains of stationary phases under T–F approximations for $c_1 = 0$. Though in the regions marked as III and IV in figure 2(a) all three types of phase separation is allowed, no cases can be found for simultaneous domain formation of all three states. One can start the analysis by first considering which of the states is energetically favored at the centre of the trap, as the condensation in an experimental situation arises first at the central region because of the density being maximum there [33]. For example in region-III where (1, 0, 0) sits at the centre of the trap, out of two possibilities of separation (0, 1, 0) wins because the separation can happen at a smaller radius than that with (0, 0, 1). Now, when (0, 1, 0) is in the outer region one can check that (0, 0, 1) never wins energetically over (0, 1, 0). To understand these, one can have a look at the phase diagrams (figure 3) on $U(r)$ versus p and $U(r)$ versus q planes. Phase separation between ferromagnetic and polar phases are observed here as one moves upward along the $U(\vec{r})$-axis at relatively larger negative q values. At a smaller negative q value, two ferromagnetic phases form domains.

Note that no possible phase separation can happen in the region marked VII and VIII. In this region the ground state will be selected depending on the chemical potential μ. As we are only concentrating on the phase separation scenario keeping a constant μ for the three unrestricted stationary states, we find (0, 0, 1) to be energetically lowest in the region I,VIII (see figure 3(a)). This situation might change when the constant μ condition is relaxed in order to find the only existing phase without any phase separation. However, that is not of our interest in this paper.

A quick comparison of this confined case can be done with the phase diagram figure 1(b) of the uniform BEC. Figure 1(b) indicates a phase separation existing for positive q, whereas, T–F approximated calculations under actual confinement gives here results in contrary to that. Figure 1(b) also indicates that there can be no phase co-existence of the two opposite ferromagnetic phases (at nonzero p), however, the confined picture reveals the opposite. This is exactly the reason one should be guided by the phase separation scenario under actual confinement rather than extrapolating density dependence of the phase in the homogeneous case to the phase separation under confinement.

3.2. Phase co-existence for $c_1 \neq 0$

The condition $c_1 \neq 0$ involves both anti-ferromagnetic and ferromagnetic interaction for $c_1 > 0$ and $c_1 < 0$ respectively. For nonzero spin interaction, it is obvious from equations (10)–(11) that the temporal variation of the different

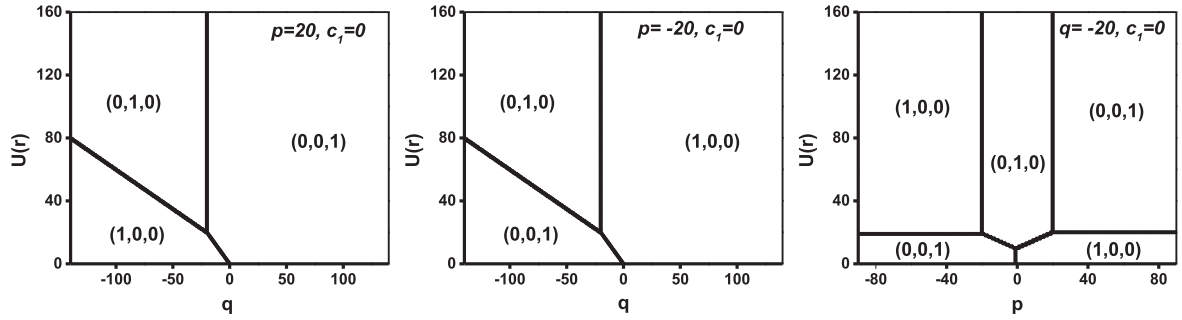

(a) $c_1 = 0$ (b) $c_1 = 0$ (c) $c_1 = 0$

Figure 3. Phase separation of a spin-1 BEC with almost no spin dependent interaction ($c_1 = 0$). (*a*) and (*b*) showing phase separation for opposite linear Zeeman terms These sub-figures are symmetric under the change of the direction of magnetic field. (*c*) Same symmetry is revealed when quadratic Zeeman term is fixed at a negative value. The phase boundaries remain unaffected with the change of chemical potential (μ). In this and all the following figures, the unit of the Zeeman terms p, q and the trapping potential $U(r)$ is Hz.

spin densities should go to zero for the stationary states. So one is left with two choices,

- at least one of the spin density is zero (corresponds to the first six states in table 2) or,
- all the subcomponents are populated but the relative phase is either 0 or π.

The stationary state corresponding to $\theta_r = 0$ with all the subcomponent densities being non-zero, is also called phase-matched (PM) state [4]. For this state, equations corresponding to all the phases are valid.

By exploiting the stationarity of phases one gets the corresponding equation for the n_0 subcomponent,

$$[U_t(\vec{r}) + c_0 n - \mu] + c_1(n_1 + n_{-1} + 2\sqrt{n_{-1}n_1}\cos\theta_r) = 0. \tag{17}$$

For further simplification one can define a parameter, $k(\vec{r}) = \sqrt{\frac{n_1}{n_{-1}}}$. Note that the ansatz (equation (9)) allows $\sqrt{n_m(\vec{r})}$ to take only positive values, negative value being accounted for by the phase factor. So by definition $k(\vec{r})$ is positive and nonzero here. The condition $\theta_r = 0$ leads to

$$[U_t(\vec{r}) + c_0 n(\vec{r}) - \mu] = -c_1[k(\vec{r}) + 1]^2 n_{-1}(\vec{r}). \tag{18}$$

Now the other two phase equations (13) become

$$U_t(\vec{r}) - p + q + c_0 n(\vec{r}) + c_1(k^2(\vec{r}) - 1)n_{-1}(\vec{r}) - \mu + c_1 n_0(\vec{r}) + c_1 n_0(\vec{r})\frac{1}{k} = 0, \tag{19}$$

$$U_t(\vec{r}) + p + q + c_0 n(\vec{r}) - c_1(k^2(\vec{r}) - 1)n_{-1}(\vec{r}) - \mu + c_1 n_0(\vec{r}) + c_1 n_0(\vec{r})k = 0. \tag{20}$$

Subtracting equation (19) from equation (20) one can express n_0 in terms of k and n_{-1},

$$c_1 n_0(\vec{r}) = \frac{-2p + 2c_1(k^2 - 1)n_{-1}(\vec{r})}{k - \frac{1}{k}}. \tag{21}$$

Similarly addition leads to another expression of n_0,

$$c_1 n_0(\vec{r}) = \frac{2c_1(k+1)^2 n_{-1}(\vec{r}) - 2q}{k + \frac{1}{k} + 2}. \tag{22}$$

Solving last two equations one gets to express $k(\vec{r})$ in terms of the external parameters p and q as, $k = \frac{q+p}{q-p}$. It is easy to see that k is positive only for $|q| > |p|$.

So, replacing the value of this k in any of the equations of n_0, and then using the equation, $n = n_0 + (k^2 + 1)n_{-1}$ we get the number densities to be

$$n_1(\vec{r}) = \frac{(p+q)^2}{4q^2}\left[n(\vec{r}) + \frac{q^2 - p^2}{2c_1 q}\right], \tag{23}$$

$$n_{-1}(\vec{r}) = \frac{(p-q)^2}{4q^2}\left[n(\vec{r}) + \frac{q^2 - p^2}{2c_1 q}\right], \tag{24}$$

$$n_0(\vec{r}) = \frac{(q^2 - p^2)}{2q^2}\left[n(\vec{r}) - \frac{q^2 + p^2}{2c_1 q}\right]. \tag{25}$$

This state corresponding to $\theta_r = 0$ is valid for the condition $|q| > |p|$ as reasoned earlier.

The total number density (defined as $n(\vec{r}) = n_1(\vec{r}) + n_0(\vec{r}) + n_{-1}(\vec{r})$) varies as

$$n(\vec{r}) = \frac{\mu - U_t(\vec{r}) + \frac{(p^2 - q^2)}{2q}}{(c_0 + c_1)}. \tag{26}$$

Corresponding energy density can be calculated by using this expression in equation (7)

$$e(\vec{r}) = U_t(\vec{r})\frac{[k_1 - U_t(\vec{r})]}{(c_0 + c_1)} + \frac{1}{2}c_0\left[\frac{k_1 - U(\vec{r})}{c_0 + c_1}\right]^2 + \frac{1}{2}c_1\left[\frac{k_1 - U(\vec{r})}{c_0 + c_1} + \frac{p^2 - q^2}{2qc_1}\right]^2, \tag{27}$$

where, $k_1 = \mu + \frac{(p^2 - q^2)}{2q}$.

The method we have used is sufficient to extract information about *APM* state ($\theta_r = \pi$) as well. We find for APM state, $k = \frac{q+p}{p-q}$. The fact that k being positive as discussed earlier ensures that $|p| > |q|$. Though these two conditions ($\theta_r = 0$ or π) lead to the same density and energy density profile of (1, 1, 1) state, the phase-matched and anti-phase-matched states exist only for the conditions $|p| < |q|$ and $|p| > |q|$ respectively.

Table 2. Density profile and T–F approximated energy density expressions for different stationary states at $c_1 \neq 0$ are shown here. The abbreviation MF stands for mixed-ferromagnetic state and (A)PM for (anti-)phase-matched state. The restrictions corresponding to MF1 and MF2 states arise automatically from the solution of equations (12) and (13). As $n_0 \geqslant 0$ both of these states are restricted in (p,q) parameter space depending on the sign of c_1.

States	Variation of density	Energy density	Restriction
(1,0,0) F1	$(c_0 + c_1)n(\vec{r}) = \mu + p - q - U(\vec{r})$	$\frac{[U(\vec{r}) - p + q][\mu + p - q - U(\vec{r})]}{(c_0 + c_1)} + \frac{[\mu + p - q - U(\vec{r})]^2}{2(c_0 + c_1)}$	none
(0,1,0) P	$c_0 n(\vec{r}) = \mu - U(\vec{r})$	$\frac{U(\vec{r})[\mu - U(\vec{r})]}{c_0} + \frac{[\mu - U(\vec{r})]^2}{2c_0}$	none
(0,0,1) F2	$(c_0 + c_1)n(\vec{r}) = \mu - p - q - U(\vec{r})$	$\frac{[U(\vec{r}) + p + q][\mu - p - q - U(\vec{r})]}{(c_0 + c_1)} + \frac{[\mu - p - q - U(\vec{r})]^2}{2(c_0 + c_1)}$	none
(1,1,0) MF1	$(c_0 + c_1)n(\vec{r}) = \mu - U(\vec{r}) + (p - q)$	$\frac{U(\vec{r})[\mu + p - q - U(\vec{r})]}{(c_0 + c_1)} + \frac{c_0[\mu + p - q - U(\vec{r})]^2}{2(c_0 + c_1)^2}$	$n_0 = \frac{p - q}{c_1}$
(1,0,1) AF	$c_0 n(\vec{r}) = \mu - q - U(\vec{r})$ and $(n_1 - n_{-1}) \equiv F_z = \frac{p}{c_1}$	$\frac{[U(\vec{r}) + q][\mu - q - U(\vec{r})]}{c_0} + \frac{[\mu - q - U(\vec{r})]^2}{2c_0} - \frac{p^2}{2c_1}$	none
(0,1,1) MF2	$(c_0 + c_1)n(\vec{r}) = \mu - U(\vec{r}) - (p + q)$	$\frac{U(\vec{r})[\mu - p - q - U(\vec{r})]}{(c_0 + c_1)} + \frac{c_0[\mu - p - q - U(\vec{r})]^2}{2(c_0 + c_1)^2}$	$n_0 = \frac{-p - q}{c_1}$
(1,1,1) (A)PM	$(c_0 + c_1)n(\vec{r}) = k_1 - U(\vec{r})$ where, $k_1 = \mu + \frac{(p^2 - q^2)}{2q}$	$\frac{U(\vec{r})[k_1 - U(\vec{r})]}{c_0 + c_1} + \frac{c_1}{2}\left[\frac{k_1 - U(\vec{r})}{c_0 + c_1} + \frac{p^2 - q^2}{2qc_1}\right]^2 + \frac{c_0}{2}\left[\frac{k_1 - U(\vec{r})}{c_0 + c_1}\right]^2$	PM($\lvert p\rvert < \lvert q\rvert$)APM ($\lvert p\rvert > \lvert q\rvert$)

Following similar scheme, subcomponent densities and energy densities corresponding to the first six states (see table 2) can be easily found out.

3.2.1. Anti-ferromagnetic interaction $c_1 > 0$. For anti-ferromagnetic type of interaction, energetic comparison of all the seven possible states along with the constraint that all the component densities are positive reveal the phase separated ground state structure. As is already mentioned, all the energy density comparison is done at a constant chemical potential (μ), ensuring chemical stability. We fix the μ at 400 nK and investigate the case for ^{23}Na , for which c_1 is positive (2.415×10^{-19} Hzm^3). The parameter c_0 is numerically 149.89×10^{-19} Hzm^3 for this element. The controllable parameters p and q can be safely varied from -150 to 150 Hz. External potential U is varied from 0 to 170 Hz. To observe the phase separation phenomenon we fix either p or q and tune the other with U.

It is obvious that for all the mixed states the subcomponent densities must be positive. This puts restrictions over p and q for all the mixed states. For example subcomponent densities for the anti-ferromagnetic state go as

$$n_{\pm 1} = \frac{\mu - q - U(\vec{r})}{2c_0} \pm \frac{p}{2c_1}. \tag{28}$$

So, AF state is only possible for the parameter value of p and q for which both of them are positive, i.e.

$$\frac{c_1}{c_0}(\mu - q - U(\vec{r}) > p > -\frac{c_1}{c_0}(\mu - q - U(\vec{r}). \tag{29}$$

This condition is similar to the restriction over p, which is $-c_1 n < p < c_1 n$, for the untrapped (homogeneous number density) case [28]. Similarly, mixed ferromagnetic and (anti-) phase-matched states have their own region of existence. Although spin–spin interaction is positive, the anti-ferromagnetic state does not win energetically to show phase coexistence, under the given setting of constant chemical potential.

Tunability of p and q and comparison of energy densities, keeping track of the above mentioned restrictions, allow us to observe many spin domain formation. At $q = 30$ Hz, if p is relaxed to a moderate negative value, a domain formation between the MF2 state, residing at the centre and F1 staying outside can be observed (figure 4(a)). A simple check, as mentioned earlier, can be helpful to see that MF2 can indeed appear in this parameter domain. Similarly, at $p = 100$ Hz, tunability of q around 48 Hz would let one observe the condensate forming a domain structure with MF1 inside and F2 outside. The magnitude of q is roughly in the same region as compared to (figure 4(a)) but p is positive in this case (not shown in figure 4). When p is fixed at 100 Hz, variation around small negative values of quadratic term reveals that a domain structure between the two ferromagnetic phase can be observed (figure 4(b)). Note that, this type of structure is not possible for untrapped situation (figure 1(a)), which reveals the novelty of the trapped condensate. For relatively smaller p, variation of q around 30.5 Hz energetically favors the PM state to occupy the high density region. F2 becomes the most stable state to capture the low density region (figure 4(c)). Obviously as $|q| > |p|$, (1, 1, 1) can be identified as a PM state. The same structure extends to larger values of p (=100 Hz) and q (101.5 to 104 Hz) which is not shown in the figure. Figure 4(d) draws one's attention to compare it with figure 4(c). Though the parameter domain in this case is different but similar structure with PM state inside and a ferromagnetic state (in this case F1) outside is observed.

Figure 5 summarizes the various possibilities of coexistence of three states that we have observed. Setting the linear term p to a small positive value, say 5 Hz, opens up the possibility to observe a domain formation of three states when q is tuned at around -61.5 Hz (figure 5(a)). The mixed ferromagnetic phase MF2 outplays all other states to stay at the low potential region. At a distance from the trap centre F1 appears as it becomes the lowest energy state. Drawing an imaginary vertical line one can find the corresponding $U(\vec{r})$, where the first phase separation happens, in turn allowing to find the domain of MF2. For 2D harmonic trap the previously defined r_0 becomes, $r_0 = \sqrt{2U/\omega}$. Following the same scheme, it is easy to find out the distance from the centre at which the next state F2 resides. Note that $(p + q)$ being negative here, it does not impose any restriction over the existence of the state MF2 (see table 2). Interesting to note that this parameter region satisfies the condition as described in equation (29). For this case, although the subcomponent number densities are positive, the AF state does not win energetically to form any domain.

For moderately small negative values of p and q another three layer domain formation can be observed (figure 5(b)). Here F1 state is only allowed to form in the most exterior part of the trap. MF2 still occupies the central region and the other ferromagnetic state F2 stays in between.

For moderately small negative p, when q is largely negative, a domain structure of two ferromagnetic state and the MF1 can be observed with F2 at the core and F1 in the most outer region are separated by a layer of MF1 (figure 5(c)).

3.2.2. Ferromagnetic interaction $c_1 < 0$. To investigate the domain formation phenomenon for ferromagnetic type of interaction we choose ^{87}Rb for which c_1 comes out to be -0.275×10^{-19} Hzm^3. The parameter c_0 is numerically 78.02×10^{-19} Hz m^3 for this element. Again all the controllable parameter and the trapping potential is varied over the specified range as stated in subsection 3.2.1. The μ is kept fixed at the value mentioned earlier. The most startling fact here is that there is no dominance of the ferromagnetic phases in the domain formation scenario as observed in this parameter region. Note that there is no apparent reason for the ferromagnetic state not to appear at all parameter regime; in fact we found out that in an extended parameter region (tuning p and q beyond ± 150 Hz) ferromagnetic state dominates in the domain formation scenario. As we are restricting ourselves in the parameter region discussed above, we are not including these cases in figure 6.

We first fix the value of the linear Zeeman term. In the parameter region as shown in figure 6(a), (0,1,0) is the most

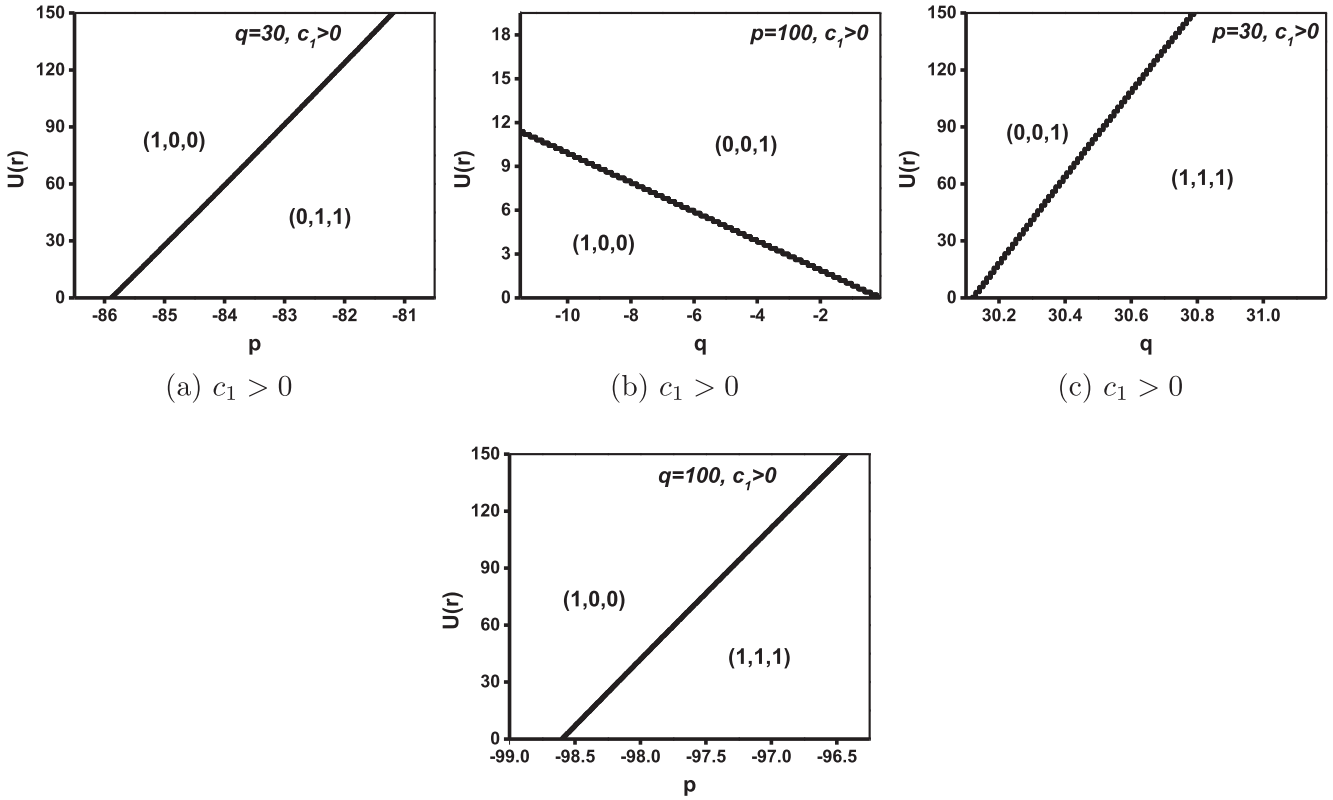

Figure 4. Possible two state coexisting structures; with (b), (c) at fixed p and (a), (d) at fixed q. Though, the interaction type is anti-ferromagnetic these domain forming structures do not include the AF state. The polar phase (0, 1, 0) also does not contribute to any phase separated structure.

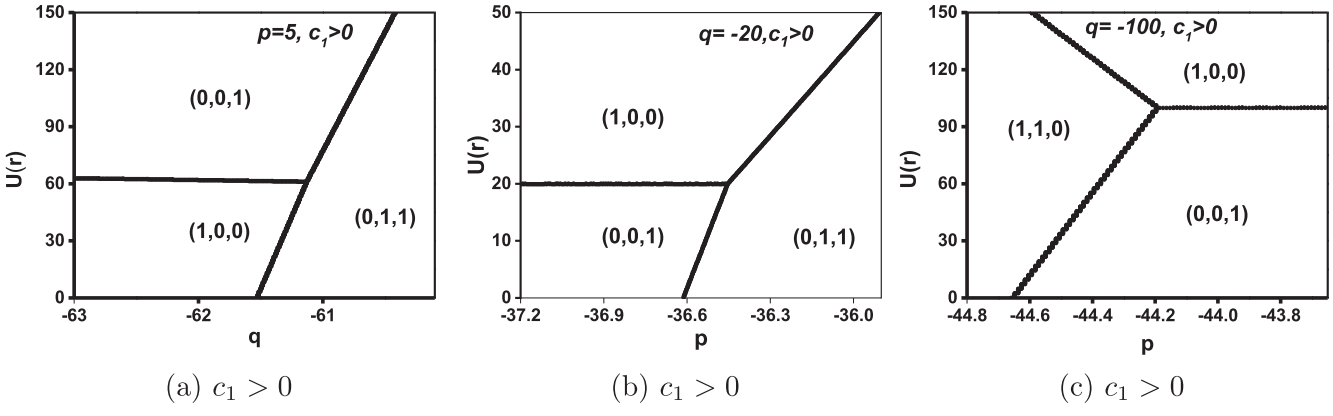

Figure 5. Domain formation possibilities with three coexisting states for different values of p and q. All these three-phase coexistence arise when q assumes a negative value. In all these structures ferromagnetic states are present. The other states that show up are mixed ferromagnetic in nature.

stable one to prevail at the outer region of the trap while the PM state stays at the core. A slight increment in the q value would only result in the broadening of the PM domain. For small p (figure 6(b)), the state (0, 1, 0) often called the polar state appears to have a phase separating structure with the AF state. Note that, this happens at a large negative value of q. For a nonzero small value of $|p|$ the polar state stays central followed by the AF state staying wide (figure 6(c)).

As the sign of q is changed, a comparison between figure 6(d) and figure 6(c) reveals the interchange of the domains of polar and AF state. In this case the AF state forms at the centre. A slight increment of $|p|$ would prefer the polar phase to expand its domain in both the cases. In this case after a limiting value of $|p|$ the structure is lost. Interesting to note that as p appears in the energy expression of the AF state (for details see the table 2) an increment in p^2 would increase the

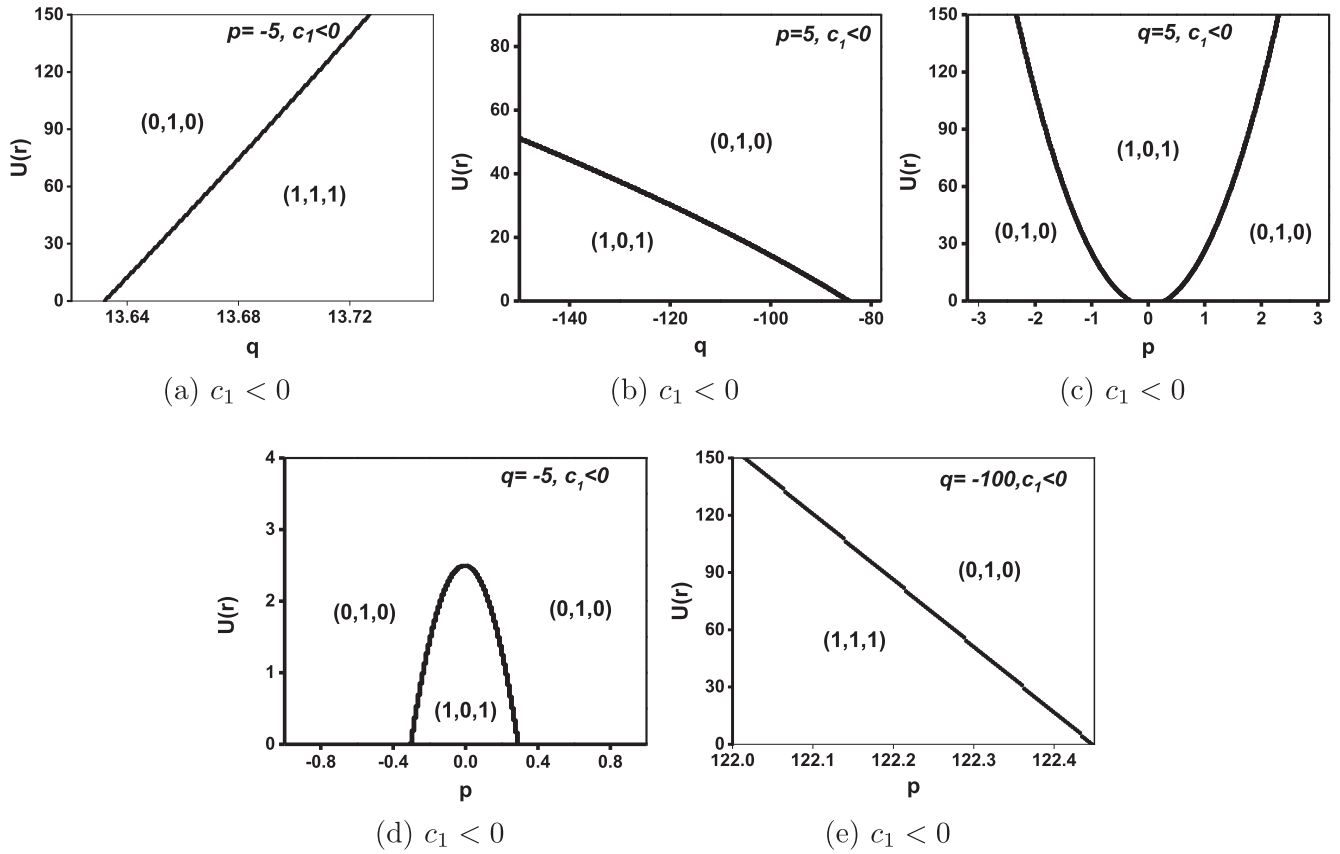

Figure 6. All possible phase separation for ferromagnetic type interaction. Only bi-layer domain structures are observed. Fixing the linear term at the specified values variation of q allows one to observe a phase separation between (a) polar and phase-matched state, (b) anti-ferromagnetic and the polar phase. For very small values of the linear Zeeman term phase separation between the polar and anti-ferromagnetic states can be observed where the quadratic term can have a small (c) positive or (d) negative value. Fixing quadratic term, variation of linear term also allows for phase separating structures between (e) anti-phase-matched and polar state and also between polar and mixed ferromagnetic state.

energy density of it for $c_1 < 0$. As p does not appear in the energy density expression of the polar state, depletion of the domain of the AF is quite reasonable to occur.

Note that, equation (7) suggests the quadratic term does not appear in the expression of energy density of the polar phase (as $m = 0$ is only present) but the AF state gets affected approximately as qn (n being the total number density). Therefore, a change in sign of q from positive (figure 6(c)) to negative (figure 6(d)) can only decrease the energy density of the AF state, thus allowing it to be energetically more stable at the high density region.

Fixing the quadratic term at $q = -100$ Hz a slight variation of the linear term around 122.25 Hz would result in the determination of a phase separating structure between the APM state and polar phase with APM state (as $|p| > |q|$) staying central. A slight increment in p will only result in the depletion of the APM domain and domination of the polar state to occupy the whole region (figure 6(e)).

3.3. Variation of individual subcomponent densities

Radial variation of subcomponent densities of the domain forming stationary states can be obtained easily following the analytical expressions provided earlier. For this purpose we assume a value of trapping frequency, $\omega = 2\pi \times 100$ Hz.

For c_0 and c_1 values corresponding to ^{23}Na , one may fix the linear and quadratic term as, $p = 5$ Hz and $q = -61.328$ Hz which would allow for a three-layer domain formation as shown in figure 5(a). The mixed-phase MF2 residing at the centre of the trap terminates at a radial distance of approximately 0.66 μm. The solid line depicting the n_0 subcomponent (figure 7(a)) is a constant for this case (see table 2), whereas, the n_1 subcomponent decreases with radial distance from the trap centre. The second layer of F1 consisting of only n_1 subcomponent exists up to an approximate distance of 0.93 μm. The other ferromagnetic phase forms the periphery consists of only n_{-1} subcomponent also decreases radially, as obvious.

Similarly for the same trapping frequency one may fix the linear and quadratic Zeeman term at 5 Hz and -133.94 Hz respectively to investigate the radial variation of sub-component number densities of a phase co-existing structure for ^{87}Rb. For this parametric values a domain forming structure between the polar and AF phase can be observed (figure 6(b)). The AF state occupying the central region vanishes at an approximate distance of 0.38 μm. As the spin–spin interaction coefficient c_1 is negative in this case the n_1 will be lesser than n_{-1} subcomponent as evident from equation (28). The outer region, covered by the polar phase

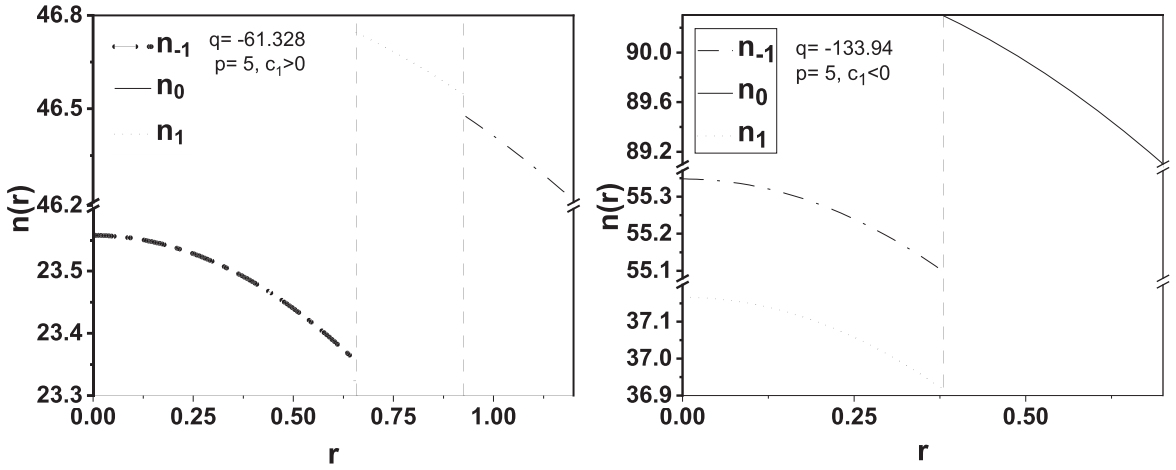

Figure 7. Radial density plots of subcomponents of different domain forming stationary states at $p = 5$ Hz and (a) $c_1 > 0$, $q = -61.328$ Hz and (b) $c_1 < 0$, $q = -133.94$ Hz. The radial distance r is scaled in μm and the number density is scaled as 10^{19} m^{-3}.

has only one subcomponent n_0 which decreases with radial distance as $-r^2$.

It is interesting to note from these two density plots that the total density variation at the interfaces of co-existing phases is not really appreciable which may be good for mechanical stability.

4. Discussion

Using T–F approximation, we have studied the phase separation of stationary states in details for a spin-1 condensate with both ferromagnetic and anti-ferromagnetic type of interaction. We show here that this procedure is indeed very general and can capture all the mixed phases equally, irrespective of the confining potential. However, the test case that has been considered in the present work makes use of an isotropic harmonic confinement. Applying optical and magnetic Feshbach resonance [34], the spin interaction parameter can be tuned [35–37] close to zero [8]. For this case also, all the possible potential induced domain structures have been investigated here in details.

The detailed analysis involving harmonic trap presented here shows a remarkable result that when interactions are ferromagnetic, the anti-ferromagnetic and polar phases dominate the domain formation scenario and for anti-ferromagnetic interaction the situation is just opposite. The actual phase boundaries can be estimated using the present analysis for any confining potential. Three-phase domain formation comes out quite naturally. We have explicitly worked out here the cases involving PM and APM phases where all the spin projections are populated to show that under T–F approximation the domain formation scenario is amenable to analytic study in general for all situation on equal footing.

It should be noted that the Zeeman terms may be varied to even higher values [38] and the scheme shown here using energy density comparison should suffice to reveal any domain structure even in that regime. At zero magnetic field the system becomes degenerate even at non-zero temperature [38]. Careful observation reveals that the energy density corresponding to the (A)PM state is ill defined at $q = 0$ (in table 2). To get rid of this issue, one can rewrite equation (12), 13 for p, $q = 0$ in the first place. It is easy to see that the subcomponent density then would be multiples of each other, a fact which agrees with the assumption taken by Gautam and Adhikari [8].

The broader picture of phase separation in terms of stationary states presented in this paper is the first step and many of the situations arising may get ruled out when a stability analysis is done with respect to density and the phase perturbations. However, this picture is essential in order to know in the beginning about all the equilibrium possibilities that can exist and about which state stability analysis should happen. The present analysis is quite interesting in that respect because it shows a complete treatment of all the phases on equal footing is possible under T–F approximation, which to our knowledge has not been done in this way in existing literature.

The present analysis also shows many new results where the actual phase boundaries over space can be obtained in the T–F approximation and the next natural step could be looking at the dynamics of those under various conditions and perturbations. These phase boundaries are places where the derivative of the order parameter cannot be neglected, however, under T–F approximation that is not the case. As a result it is essential that the stability analysis around each and every phase boundary of domains be done and we would in future look into this to see if any general stability condition can be arrived at. The constant chemical potential constraint which is essential for chemical stability of coexisting phases may also be a heavy requirement for many cases under various conditions and the failure of maintaining this constraint may also rule out some otherwise allowed structures. Nevertheless, the broader picture of stationary phase separated domains is necessary and the present analysis will help in that purpose.

Acknowledgments

PKK would like to thank the Council of Scientific and Industrial Research (CSIR), India for the funding provided and Sourav Laha for many helpful discussion.

ORCID iDs

Projjwal K Kanjilal https://orcid.org/0000-0002-1003-9166
A Bhattacharyay https://orcid.org/0000-0002-7976-0760

References

[1] Timmermans E 1998 Phase separation of Bose–Einstein condensates *Phys. Rev. Lett.* **81** 5718–21
[2] Stenger J, Inouye S, Stamper-Kurn D M, Miesner H-J, Chikkatur A P and Ketterle W 1998 Spin domains in ground-state Bose–Einstein condensates *Nature* **396** 345–8
[3] Isoshima T, Machida K and Ohmi T 1999 Spin-domain formation in spinor Bose–Einstein condensation *Phys. Rev.* A **60** 4857–63
[4] Matuszewski M 2010 Ground states of trapped spin-1 condensates in magnetic field *Phys. Rev.* A **82** 053630
[5] Matuszewski M, Alexander T J and Kivshar Y S 2008 Spin-domain formation in antiferromagnetic condensates *Phys. Rev.* A **78** 023632
[6] Matuszewski M, Alexander T J and Kivshar Y S 2009 Excited spin states and phase separation in spinor Bose–Einstein condensates *Phys. Rev.* A **80** 023602
[7] Swisłocki T and Matuszewski M 2012 Controlled creation of spin domains in spin-1 Bose–Einstein condensates by phase separation *Phys. Rev.* A **85** 023601
[8] Gautam S and Adhikari S K 2015 Analytic models for the density of a ground-state spinor condensate *Phys. Rev.* A **92** 023616
[9] Jiménez-García K, Invernizzi A, Evrard B *et al* 2019 Spontaneous formation and relaxation of spin domains in antiferromagnetic spin-1 quasi-condensates *Nat Commun* **10** 1422
[10] Ho T-L and Shenoy V B 1996 Binary mixtures of bose condensates of alkali atoms *Phys. Rev. Lett.* **77** 3276–9
[11] Sabbatini J, Zurek W H and Davis M J 2011 Phase separation and pattern formation in a binary Bose–Einstein condensate *Phys. Rev. Lett.* **107** 230402
[12] Vidanović I, van Druten N J and Haque M 2013 Spin modulation instabilities and phase separation dynamics in trapped two-component Bose condensates *New J. Phys.* **15** 035008
[13] Gautam S and Angom D 2011 Phase separation of binary condensates in harmonic and lattice potentials *J. Phys. B: At. Mol. Opt. Phys.* **44** 025302
[14] Lee K L, Jørgensen N B, Liu I-K, Wacker L, Arlt J J and Proukakis N P 2016 Phase separation and dynamics of two-component Bose–Einstein condensates *Phys. Rev.* A **94** 013602
[15] Liu Z 2009 Phase separation of two-component Bose–Einstein condensates *J. Math. Phys.* **50** 102104
[16] Tojo S, Taguchi Y, Masuyama Y, Hayashi T, Saito H and Hirano T 2010 Controlling phase separation of binary Bose–Einstein condensates via mixed-spin-channel feshbach resonance *Phys. Rev.* A **82** 033609
[17] Zhu L and Li J 2017 Phase separation of two-component Bose–Einstein condensates with monopolar interaction *Mod. Phys. Lett.* B **31** 1750215
[18] Wen L, Liu W M, Cai Y, Zhang J M and Hu J 2012 Controlling phase separation of a two-component Bose–Einstein condensate by confinement *Phys. Rev.* A **85** 043602
[19] Xi K-T, Li J and Shi D-N 2011 Phase separation of a two-component dipolar Bose–Einstein condensate in the quasi-one-dimensional and quasi-two-dimensional regime *Phys. Rev.* A **84** 013619
[20] Bandyopadhyay S, Roy A and Angom D 2017 Dynamics of phase separation in two-species Bose–Einstein condensates with vortices *Phys. Rev.* A **96** 043603
[21] Wen L, Sun Q, Wang H Q, Ji A C and Liu W M 2012 Ground state of spin-1 Bose–Einstein condensates with spin–orbit coupling in a zeeman field *Phys. Rev.* A **86** 043602
[22] Wang C, Gao C, Jian C-M and Zhai H 2010 Spin–orbit coupled spinor Bose–Einstein condensates *Phys. Rev. Lett.* **105** 160403
[23] Gautam S and Adhikari S K 2014 Phase separation in a spin–orbit-coupled Bose–Einstein condensate *Phys. Rev.* A **90** 043619
[24] Li J, Yu Y-M, Jiang K-J and Liu W-M 2018 Phase separation and hidden vortices induced by spin–orbit coupling in spin-1 Bose–Einstein condensates arXiv:1802.00138
[25] Bhuvaneswari S, Nithyanandan K and Muruganandam P 2018 Spotlighting phase separation in rashba spin–orbit coupled Bose–Einstein condensates in two dimensions *J. Phys. Commun.* **2** 025008
[26] Stamper-Kurn D M, Andrews M R, Chikkatur A P, Inouye S, Miesner H-J, Stenger J and Ketterle W 1998 Optical confinement of a Bose–Einstein condensate *Phys. Rev. Lett.* **80** 2027–30
[27] Ho T-L 1998 Spinor bose condensates in optical traps *Phys. Rev. Lett.* **81** 742–5
[28] Kawaguchi Y and Ueda M 2012 Spinor Bose–Einstein condensates *Phys. Rep.* **520** 253–381
[29] Qi R, Yu X-L, Li Z B and Liu W M 2009 Non-abelian josephson effect between two $f = 2$ spinor Bose–Einstein condensates in double optical traps *Phys. Rev. Lett.* **102** 185301
[30] Barrett M D, Sauer J A and chman M S 2001 All-optical formation of an atomic Bose–Einstein condensate *Phys. Rev. Lett.* **87** 010404
[31] Ohmi T and Machida K 1998 Bose–Einstein condensation with internal degrees of freedom in alkali atom gases *J. Phys. Soc. Jpn.* **67** 1822–5
[32] Ji A-C, Liu W M, Song J L and Zhou F 2008 Dynamical creation of fractionalized vortices and vortex lattices *Phys. Rev. Lett.* **101** 010402
[33] Proukakis N 2013 *Quantum Gases: Finite Temperature and Non-equilibrium Dynamics* vol 1 (Singapore: World Scientific)
[34] Moerdijk A J, Verhaar B J and Axelsson A 1995 Resonances in ultracold collisions of ^{6}Li, ^{7}Li, and ^{23}Na *Phys. Rev.* A **51** 4852–61
[35] Inouye S, Andrews M R, Stenger J, Miesner H-J, Stamper-Kurn D M and Ketterle W 1998 Observation of feshbach resonances in a Bose–Einstein condensate *Nature* **392** 151
[36] Chin C, Grimm R, Julienne P and Tiesinga E 2010 Feshbach resonances in ultracold gases *Rev. Mod. Phys.* **82** 1225–86
[37] Liang Z X, Zhang Z D and Liu W M 2005 Dynamics of a bright soliton in Bose–Einstein condensates with time-dependent atomic scattering length in an expulsive parabolic potential *Phys. Rev. Lett.* **94** 050402
[38] Frapolli C, Zibold T, Invernizzi A, Jiménez-García K, Dalibard J and Gerbier F 2017 Stepwise Bose–Einstein condensation in a spinor gas *Phys. Rev. Lett.* **119** 050404